

Adsorption of antimony on Au(001)

G. K. Wertheim, J. E. Rowe, D. N. E. Buchanan, and H. L. Polite
AT&T Bell Laboratories, Murray Hill, New Jersey 07974-2070

H. Shigekawa*

Department of Physics, University of Florida, Gainesville, Florida 32611

(Received 31 May 1988)

Antimony overlayers on a clean Au(001) surface were prepared by surface segregation on a sputtered and annealed, Sb-doped gold single crystal. Valence-band photoemission data, taken with photon energies between 35 and 150 eV, exhibit a Sb $5p$ contribution at the Fermi energy at the higher photon energies. Core-level photoemission data yield surface-atom shifts for the Au $4f$ core electrons of +0.44 and +0.90 eV, opposite in sign to that of the clean Au surface, and suggestive of loss of charge from the Au surface layer. Sb $4d$ core-level spectra have the asymmetric line shape associated with metallic screening with a many-body singularity index of 0.08. This value is significantly larger than that of bulk gold, and suggests screening by electrons in Sb-derived states at the Fermi level. All aspects of these measurements indicate that the Sb is strongly chemisorbed and probably forms an ordered surface alloy. The reconstruction of the Sb-covered surface was investigated by low-energy electron diffraction, and showed a compressed hexagonal layer with 4×22 periodicity, which fits a modified (111) double layer of AuSb₂ with a small number of additional reconstructed Au atoms.

INTRODUCTION

Overlayer systems are most commonly prepared by the controlled deposition of foreign atoms on a clean surface, but it is well known that surface segregation from the bulk offers an alternate route. The latter process is particularly attractive because surface contamination is minimized and a thermally equilibrated surface structure is formed. The interaction of Au and Sb is of some interest because it has relevance to the nature of the interface formed between gold metallization and an antimonide III-V-compound semiconductor substrate. In particular, if the interaction between Au and Sb is sufficiently strong, one can anticipate the disruption of the III-V bonds to form Au—Sb bonds. The high heat of formation of the familiar AuX₂ (X = Al, Ga, or In) compounds then suggests that Au, rather than acting like an inert noble metal, may well form compounds with both components of the semiconductor, seriously disrupting the interface. The surface segregation is relevant to the use of Sb-doped Au in making contacts to n -type semiconductors in general. Strong segregation of Sb to the Au-semiconductor interfaces may facilitate the diffusion of Sb into the semiconductor, which promotes the formation of an Ohmic contact.

The maximum solid solubility of Sb in Au is of the order of 1 at %.¹ According to the analysis of Miedema² and its extension by Chelikowsky,³ antimony has a strong tendency to segregate to the surface with a segregation coefficient of several thousand. Our measurements support this and suggest that the surface concentration may be $\sim 10^4$ relative to the bulk.

EXPERIMENTAL DETAILS

The Sb overlayer system was prepared by annealing a Sb-doped Au single crystal which had been oriented to within $\pm 1^\circ$ and cut to expose a (100) surface. The polished surface of the gold crystal was first cleaned by sputtering with Ar ions until both carbon and oxygen Auger signals had become negligible. Neither Auger nor photoemission data from this sputtered surface gave a detectable Sb signal. X-ray-fluorescence measurements⁴ gave a limit for the bulk Sb concentration of less than 10^{-4} . The sputtered sample was then heated to 600–750 °C by back-surface electron bombardment to remove the sputter-etching damage and to make the dilute bulk antimony segregate to the surface. This treatment resulting in a surface with reproducible Sb coverage and low-energy electron-diffraction (LEED) pattern. The LEED measurements showed a complex but well-ordered surface. The periodicity appears to be 4×22 with two domains rotated by 90° as expected for a (100) surface. The Sb coverage was most effectively monitored by photoemission, because the sharp Sb $4d$ doublet has a large photoelectric cross section⁵ and is well separated from other signals, see Fig. 1. In Auger spectra excited by 3-keV electrons the Sb response is less apparent, but can be readily identified. Using published Auger sensitivity factors, the Sb concentration is less than $\frac{1}{2}$ monolayer, with an uncertainty of $\sim 50\%$ due to resolution differences between our data and the handbook spectra.⁶

The photoemission studies were done on the AT&T Bell Laboratories 6-m toroidal-grating-monochromator beam line U4A at the National Synchrotron Light Source

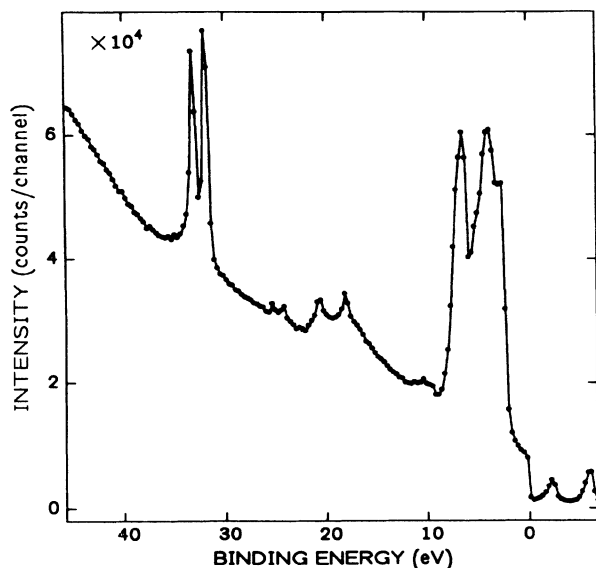


FIG. 1. Wide-scan photoemission spectrum of Au(001) with Sb overlayer prepared by surface segregation. The photon energy is 90 eV.

at Brookhaven National Laboratory (Upton, NY). The photoemission data were taken with a Vacuum Science Workshop 100-mm hemispherical electron-energy analyzer.

RESULTS AND DISCUSSION

A wide-scan photoemission spectrum obtained with 90-eV radiation from a freshly prepared surface is shown in Fig. 1. The lines near 32 eV are the Sb 4*d* spin-orbit doublet, the band between 2 and 8 eV the Au 5*d* states, and the complex of lines near 20 eV the Au *NOO* Auger electrons with peaks at 69 and 72 eV kinetic energy. The lines just above E_F are due to emission from the Au 4*f* states, excited by second-order radiation. The Sb coverage can be readily estimated from the areas of the Sb 4*d* and Au 5*d* components, using the cross sections of Yeh and Lindau.⁵ Assuming an escape depth of 6 Å,⁷ the resulting coverage is $\Theta=0.29$, with an uncertainty, based on those of the measured areas, large enough to encompass coverages of both $\frac{1}{4}$ and $\frac{1}{3}$ monolayers. This estimate is, of course, a strong function of the escape depth, and coverages up to $\frac{1}{2}$ monolayer are not inconsistent with the data, if the actual escape depth is significantly smaller.

Valence-band spectra

Valence-band spectra taken over a range of energies are shown in Fig. 2. At the lowest photon energies the photoemission intensity is due almost exclusively to the Au 5*d* states. Below 100 eV the Au 6*s* and Sb 5*p* cross sections are 2 or 3 orders of magnitude smaller than that of the Au 5*d* states. The 6*s* conduction band is visible largely by virtue of its Au 5*d* admixture. At 150 eV, the

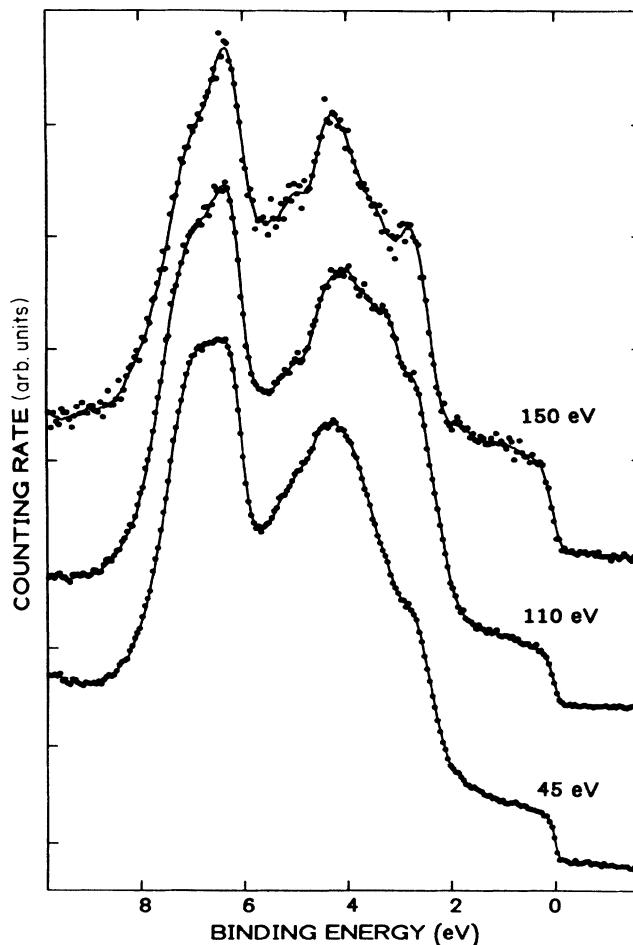


FIG. 2. Valence-band spectra of the Sb on Au(001) overlayer system at the three photon energies indicated. Note the increase in the response near E_F with increasing photon energy.

Au 5*d* cross section has dropped to 0.24 Mb, approaching its Cooper minimum of 0.10 Mb, while that of Sb 5*p* is still 0.06 Mb. Some of the features of the valence-band spectrum must now reflect Sb 5*p* contributions. The increase in the intensity of the conduction-band photoemission for 0–2 eV binding energy is the major contribution attributable to the Sb 5*p* admixture into the surface conduction band. This admixture is confirmed by the core-level results discussed in the next subsection.

Core-level binding-energy shifts

The core-level spectra of both the surface Sb and the substrate Au were also examined in greater detail. The Sb 4*d* data were taken with a takeoff angle of 45° to enhance the surface sensitivity, and a photon energy of 90 eV. For energies closer to the 60-eV maximum in the Sb 4*d* photoionization cross section, emission from the Au 4*f* states excited by second-order light would fall into the region of interest.

The high-resolution Sb 4*d* spectrum in Fig. 3 has been fitted with a spin-orbit doublet having Doniach-Šunjić⁸

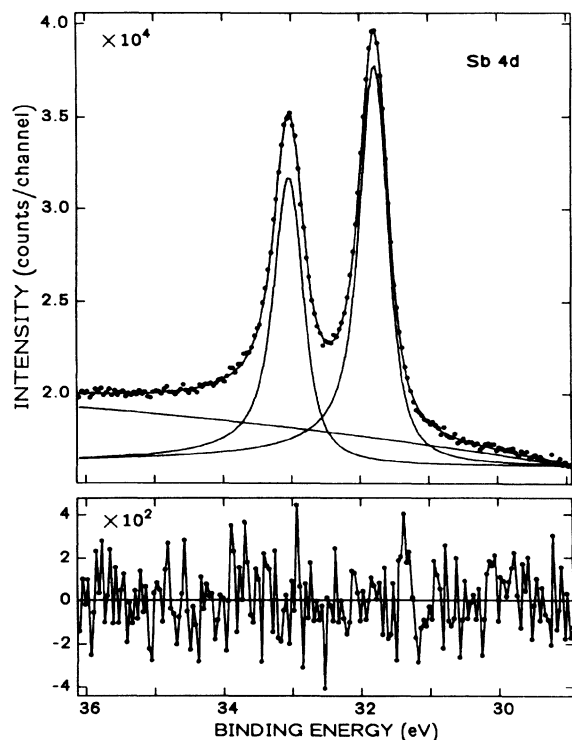


FIG. 3. Least-squares fit to the Sb 4*d* photoemission spectrum of the overlayer system in Fig. 1. The residuals are shown below, vertically magnified by a factor of 12. The photon energy is 90 eV.

line shape and a quadratic background. The spin-orbit splitting is 1.248 ± 0.004 eV, in very good agreement with earlier x-ray-photoemission-spectroscopy results.⁹ The binding energy of the $4d_{5/2}$ component is 31.76 eV, slightly smaller than the value for elemental Sb, 32.14 eV,⁹ as is commonly observed for anions in compounds. From the simplest point of view, this indicates charge transfer to the antimony. The lifetime width of the 4*d* lines is 0.28 eV, significantly larger than that recently determined for the neighboring element Sn, 0.23 eV.¹⁰ A larger width is expected for Sb not only because of the increased *d*-electron binding energy, but also because of the increased 5*p* occupancy that promotes the $N_{IV,V}O_{II,III}O_{II,III}$ Auger transition.

The singularity index of 0.08 is greater than that of metallic gold, 0.04,¹¹ i.e., the adsorbate Sb core hole is more effectively screened than a Au core hole in the metallic substrate. It seems unlikely that this can be accomplished by electrons in the Au 6*s* conduction band, and can be understood only if there are Sb-derived states at E_F to screen the Sb core hole. In other words, the observation that the singularity index of the adsorbate is greater than that of the substrate requires that there be adsorbate states in a conduction band at E_F , in agreement with the interpretation of the valence-band data in

Fig. 2.

The Gaussian width of 0.29 eV is larger than that expected on the basis of the combined monochromator and spectrometer resolutions, which is estimated to be ~ 0.18 eV. Phonon or inhomogeneous broadening amounting to ~ 0.23 eV must therefore be present. Phonon broadening is unlikely to be of this magnitude in a metallic system. Since the residuals of the fit in Fig. 3 do not exhibit any systematic fluctuations, it is clear that the excess width is not due to a simple splitting into two unresolved components. It seems likely that the broadening is due to a large number of inequivalent sites. We return to this point in the discussion of the LEED patterns.

The high-resolution Au 4*f* data in Fig. 4 were taken with a photon energy of 170 eV. The data could not be adequately fitted with fewer than three components [with identical Doniach-Šunjić (DS) shape] on a linear background. In the line-shape fitting procedure each component was represented by a spin-orbit doublet, because the tails of the $4f_{5/2}$ lines contribute to the line shape near 86 eV. In the figure the linear background determined by the fitting procedure has been subtracted to display the line shape more clearly. The major component at 84 eV is due to gold in the bulk, the components at greater binding energy due to gold on the surface. The shifts are 0.44 and 0.90 eV, and the intensities as fractions of those of the main line are 0.38 and 0.09, respectively. [In contrast, the surface-atom core-level shift of a reconstructed Au(001)-(5 × 20) surface is -0.28 eV, i.e., toward smaller binding energy.^{11,12}] The sign of the present shifts are indicative of loss of electronic

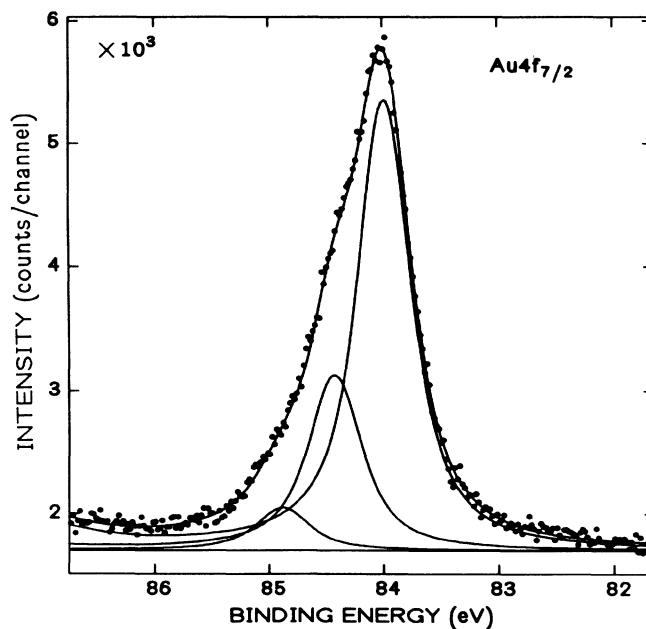


FIG. 4. Least-squares analysis of the Au $4f_{7/2}$ photoemission-line spectrum of a sample like that in Fig. 1. The data are fitted with three components of identical shape, and a parabolic background, but are shown with the background subtracted. The photon energy is 170 eV.

charge to the adsorbate. The fractional intensity associated with a full surface monolayer, for an escape depth of 6 Å and a takeoff angle of 45°, is 0.62. The two observed components, consequently, correspond to coverages of 0.61 and 0.15 monolayers. The interpretation of these intensities depends on the surface morphology, and will be given in the context of the LEED analysis.

LEED analysis

Low-energy electron diffraction was performed with a commercial display apparatus¹³ which had been modified to allow viewing from either the sample side or the display-screen side (rear-view LEED). The LEED patterns were quite distinct only at low energies, below 30 eV, and showed a rather complex array of LEED beams, as seen in Fig. 5. The specular (00) beam appears in the lower left of each photograph. In addition, there are two strong beams at $\pm 30^\circ$ from the vertical and horizontal, which belong to two equivalent hexagonal domains rotated $\pm 90^\circ$, as expected for a (100) surface with a reconstructed pattern of less than fourfold rotational symmetry. The surface lattice constant of this reflection is 4.37 Å for a hexagonal (111)-type two-dimensional layer and this value is close to that of the bulk (111) planes of AuSb₂.¹⁴ Following the procedures used for reconstructed clean Au(100), one can assign the LEED beams to one of three sources: (a) the Au(100) substrate, (b) the hexagonal overlayer, or (c) interaction beams due to multiple scattering between the overlayer and substrate.¹⁵ A dia-

gram of such a multiple-scattering interpretation of our LEED patterns is shown in Fig. 6, where only the multiple-scattering beams with two or three combinations of overlayer and substrate reciprocal-lattice vectors are shown.

The symmetry of these LEED patterns is markedly different from the typical hexagonal overlayers previously observed on (100) substrates Ref. 16 in that the strong reflections are not along the principal $\langle 001 \rangle$ -type directions in the surface plane, but instead are both along these directions and also along the hexagonal directions inclined at 30° to the $\langle 011 \rangle$ -type fourfold directions. This is, in part, due to the larger difference in lattice constant ratio of the hexagonal overlayer and substrate Au(100) as compared to the clean surface. However, this intensity distribution and the appearance of strong diffraction only at relatively low electron energy suggest that the hexagonal layer which gives the reconstructed LEED pattern is more than 1 monolayer thick. In fact, one can give a probable explanation of both the LEED and photoelectron spectra with a hexagonal overlayer of a modified (111) double layer of AuSb₂. Figure 7 shows one such modified double layer, which has 1.21×10^{15} cm⁻² Au atoms with 6.1×10^{14} cm⁻² Sb atoms in a plane above the Au atoms. The density of Au atoms is about 10% smaller than on the clean 5×20 Au(100) surface, which also has a hexagonal Au overlayer. However, the nearest-neighbor in-plane Au spacing for a strictly planar Au layer and planar Sb layer is 12.5% shorter than that of clean Au(100). Thus we might expect some distortion

HEXAGONAL Sb/Au (100)

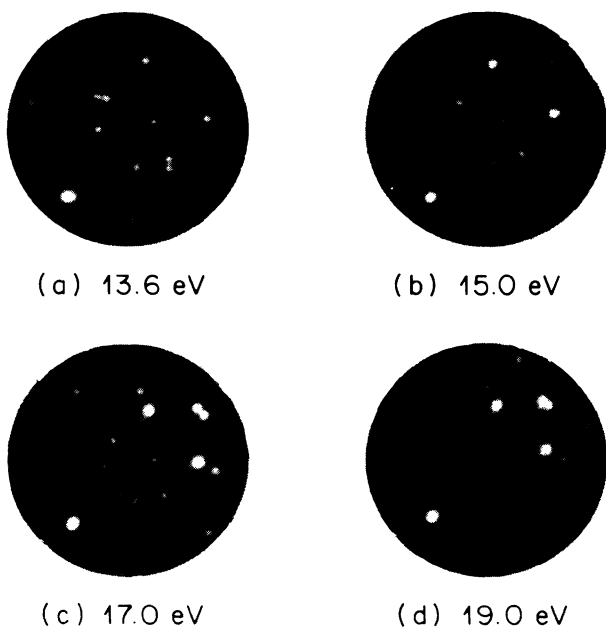


FIG. 5. Photographs of LEED patterns measured for Au(100) with Sb overlayer as described in the text for electron energies of 13.6, 15.0, 17.0, and 19.0 eV.

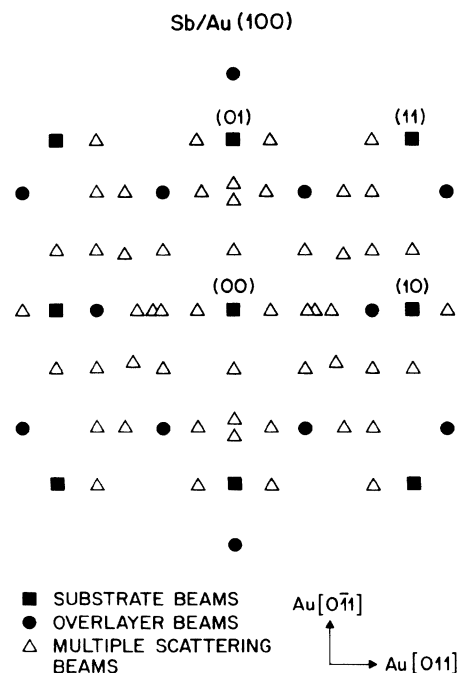


FIG. 6. Diagram of the LEED patterns shown in Fig. 5 with the substrate beams (■), overlayer beams (●), and multiple-scattering beams (△) separately identified. Only one of the two equivalent 90° domains is shown.

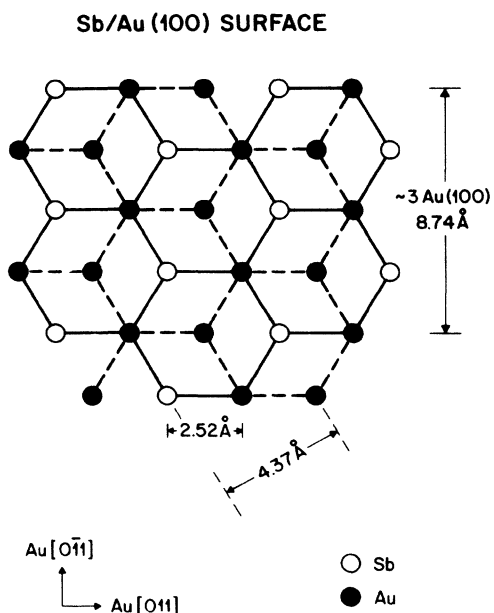


FIG. 7. Model for the hexagonal double layer of Sb-Au on the Au(100) surface with a coincidence lattice between two unit meshes of this structure and three unit meshes of the substrate Au(100) lattice.

(perhaps buckling) of these planes which would produce several inequivalent Sb sites consistent with the photoemission linewidths discussed above.

The hexagonal lattice constant of bulk AuSb_2 is 4.67 \AA , which is 7.6% larger than the surface lattice constant; this difference allows a coincidence between the substrate Au(100) layer (assumed bulklike) and the modified AuSb_2 overlayer in a ratio of 3:2. The strain associated with this changes the apparent periodicity from 5×20 of the clean Au(100) to 4×22 for the Sb-overlayer-covered Au(100). The hexagonal surface layers are incomplete possibly due to strain effects and thus cover only 0.7 ± 0.1 of the surface area. The Sb interacts strongly with the surface Au in the modified AuSb_2 hexagonal layer which gives rise to the 4×22 LEED pattern. The weaker Au $4f$ component at 84.90 eV binding energy can be assigned to additional Au atoms (not shown in Fig. 7) above the Sb layer in the modified AuSb_2 configuration. These additional Au atoms may have larger charge transfer to the Sb atoms than the other surface Au atoms due to a lower number of Au neighbors. The photoemission intensity ratio for the hexagonal surface layer to bulk signal¹² for clean Au(100) is 0.87 which is 2.3 times larger than the intensity ratio we observe which is due in part to a smaller es-

cape depth (i.e., different photon energy), but may also indicate that the hexagonal overlayer for their samples consisted of more than one monolayer.

CONCLUSIONS

These measurements show that Sb forms a well-ordered, compressed hexagonal layer with 4×22 periodicity on Au(001). The presence of two different types of surface Au detected by photoemission as well as the strong energy dependence of the LEED pattern intensities suggests that the overlayer is at least 2 atomic layers thick. It probably consists of a hexagonal Au-Sb layer which covers about 0.6–0.8 of the surface area based on photoemission core-level intensities and an escape depth of 6 Å. This layer has a structure similar to that of a (111) double layer of AuSb_2 as shown in Fig. 6 with some additional Au atoms. The photoemission measurements support this interpretation and show that there is a suitable amount of Sb on the surface to form this configuration with an additional number of surface Au atoms. The shift of both surface Au $4f$ lines to larger binding energy (opposite to clean Au) shows that the surface Sb interacts chemically with both types of surface gold atoms. We conclude that the overlayer is metallic on the basis of the asymmetric photoelectron line shape observed. From the chemical shifts of the surface Au $4f$ lines, the intensity of the Sb $5p$ signal near E_F and the surface lattice constant determined from LEED, we conclude that there is a strong interaction between the surface Au and Sb atoms. It may be more correct to describe the reconstructed overlayer as a surface alloy rather than a strained AuSb_2 layer since the surface composition shows a larger number of Au atoms than for the stoichiometric compound. This rather complex overlayer system may be of interest to workers in the field of He-atom diffraction. Since the thermal He-atom beam does not penetrate the surface layer, the diffraction could be simplified by the absence of the multiple-scattering LEED beams that we see. One would then observe only a superposition of diffraction patterns from the hexagonal domains and the uncovered substrate portions of the surface.

ACKNOWLEDGMENTS

This work was carried out in part at the National Synchrotron Light Source, Brookhaven National Laboratory, which is supported by the U.S. Department of Energy (Division of Materials Sciences and Division of Chemical Sciences of the Office of Basic Energy Sciences), under DOE Contract No. DE-AC02-76CH00016.

*On leave from Department of Applied Physics, University of Tokyo, Tokyo 113, Japan.

¹M. Hansen and K. Anderko, *Constitution of Binary Alloys* (McGraw-Hill, New York, 1958), p. 230.

²A. R. Miedema, *Z. Metallkd.* **69A**, 455 (1978).

³J. R. Chelikowsky, *Surf. Sci.* **139**, L197 (1984), and private

communication.

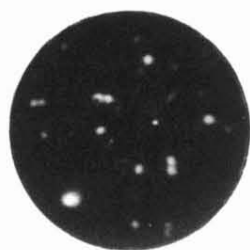
⁴N. D. Hobbins (private communication).

⁵J. J. Yeh and I. Landau, *At. Data Nucl. Data Tables* **32**, 1 (1985).

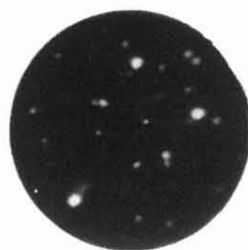
⁶L. E. Davis, N. C. MacDonald, P. W. Palmberg, G. E. Riach, and R. E. Weber, *Handbook of Auger Electron Spectroscopy*

- (Physical Electronics Division, Perkin-Elmer, Eden Prairie, MN, 1976), pp. 5–18.
- ⁷C. R. Brundle, *Surf. Sci.* **48**, 99 (1975).
- ⁸S. Doniach and M. Šunjić, *J. Phys. C* **3**, 385 (1970).
- ⁹R. A. Pollak, S. A. P. Kowalczyk, L. Ley, and D. A. Shirley, *Phys. Rev. Lett.* **29**, 274 (1972).
- ¹⁰Earlier XPS work gave a value of 0.22 eV; see G. K. Wertheim and S. Hüfner, *Phys. Rev. Lett.* **35**, 53 (1975).
- ¹¹P. H. Citrin, G. K. Wertheim, and Y. Baer, *Phys. Rev. Lett.* **41**, 1425 (1978); *Phys. Rev. B* **27**, 3160 (1983).
- ¹²P. Heinmann, J. F. van der Veen, and D. E. Eastman, *Solid State Commun.* **38**, 595 (1981).
- ¹³Physical Electronics Division, Perkin Elmer, Eden Prairie, MN.
- ¹⁴A. R. Graham and S. Kaiman, *Am. Mineral.* **37**, 416 (1952).
- ¹⁵P. W. Palmberg and T. N. Rhodin, *J. Chem. Phys.* **9**, 147 (1968).
- ¹⁶P. W. Palmberg and T. N. Rhodin, *J. Chem. Phys.* **9**, 134 (1968).

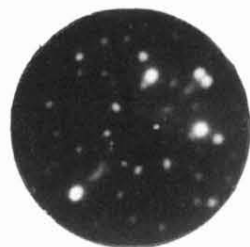
HEXAGONAL Sb/Au (100)



(a) 13.6 eV



(b) 15.0 eV



(c) 17.0 eV



(d) 19.0 eV

FIG. 5. Photographs of LEED patterns measured for Au(100) with Sb overlayer as described in the text for electron energies of 13.6, 15.0, 17.0, and 19.0 eV.